Electronic Supplementary Information (ESI)

Scalable and continuous nanomaterial integration with transgenic fibers for enhanced photoluminescence

Jung Woo Leem[1,†] , Seung Ho Choi[1,†], Seong-Ryul Kim[2], Seong-Wan Kim[2],

Kwang-Ho Choi[2,*], and Young L. Kim[1,3,4,*]

[1]Weldon School of Biomedical Engineering, Purdue University, West Lafayette, IN 47907, USA
[2]Department of Agricultural Biology, National Academy of Agricultural Science, Rural Development Administration, Jeonju, Jeollabuk-do 54875, South Korea
[3]Department of Computer Science and Engineering, Kyung Hee University, Yongin, Gyeonggi-do 17104, South Korea
[4]Purdue Quantum Center, Purdue University, West Lafayette, IN 47907, USA

* To whom correspondence should be addressed

E-mail: ckh@korea.kr (Dr. K. H. Choi) and youngkim@purdue.edu (Prof. Y. L. Kim)

[†]J. W. Leem and S. H. Choi are contributed equally to this work.

Reflectance and fluorescence confocal microscopy measurements

In addition to electron microscopy and energy dispersive X-ray, we made extensive use of reflectance confocal microscopy (RCM) to directly visualize AgNPs embedded inside silk fibers. The typical configuration of RCM can be summarized as follows: confocal aperture size = 50 or 80 μm (i.e., ~ 0.5 airy unit), numerical aperture = 0.4, and scan speed (pixel dwell time) = 10 μs/pixel. For optically sectioned images, we generated 2D RCM images of AgNP-embedded silk under three different illumination wavelengths of 488, 543, and 633 nm on the same optically sectioned plane. For 3D visualizations, we stacked 64 image slices with a slice thickness of 0.2 μm along the z-axis (total thickness = 12.6 μm), covering an area up to ~ 211.7 × 211.7 μm^2. For fluorescence (mKate2) confocal images, we used a laser excitation source at 543 nm and a detection bandpass of 600 – 700 nm.

Mechanical property measurements

We explored the integration effect of AgNPs into silk fibers on the mechanical properties. For each silk cocoon, at least 15 single fibers were tested. A universal electromechanical test machine (100P/Q, TestResources) was used with an extension rate of 1 mm min^{-1} and a gauge length of 10 mm under ambient conditions (25 ± 2 °C and 50 ± 10% relative humidity). There were no significant variations in the diameter of AgNP-embedded silk fibers compared to the native bare silk fibers before the integration of AgNPs, measured under an optical microscope. As shown in Table S2 and Fig. S9, after AgNP hybridization with silk, the common mechanical properties of individual silk fibers, including the maximum strain, the maximum stress, and the Young's modulus, were not significantly changed. A one-way ANOVA test showed that the three groups of the Young's moduli (i.e., native bare control silk fibers and AgNP-embedded silk fibers at 0.5-mM $AgNO_3$ and 1.0-mM $AgNO_3$) were not different statistically with a p-value of 0.3. Thus, the integration of AgNPs into silk did not

lead to considerable variations in the mechanical properties of individual silk fibers. We note that the previous studies have reported the maximum strain and stress values of degummed silk fibers in wide ranges of 4 − 26% and 300 − 600 MPa, respectively.[1-3] Such large variations for different samples are often caused by different feeding environments, degumming processes, testing parameters, and analysis methods. In our analyses, we only investigated the integration effect of AgNPs into silk fibers on the mechanical properties using degummed silk cocoons under the same conditions.

Mass density of mKate2/Fibroin H-chain fusion recombinant protein

We estimated the mass density of mKate2/Fibroin H-chain fusion recombinant protein in the transgenic silk cocoon as ~ 12.6 %. Using quantitative densitometry of SDS/PAGE, we measured the protein SDS/PAGE spot optical density, which is proportional to the mass of the expressed fusing protein. 25 mg of each cocoon shell was dissolved in 1 mL of 60% (w/v) lithium thiocyanate by vortex-mixing for 10 minutes and was incubated at room temperature for 1 hour followed by centrifugation at 10,000 rpm in a microcentrifuge for five minutes. 5-μL samples were subjected to SDS/PAGE [10% (w/v) polyacrylamide slab gel] by dissolving in an equal volume of a sample loading buffer [5% (v/v) glycerol, 1% (w/v) SDS, 0.05% (w/v) bromophenol blue, 0.0625 M Tris/HCl, pH 6.8] with 2% (v/v) 2-mercaptoethanol and were boiled for five minutes. After electrophoresis, the gel was stained with a staining buffer [0.1% (w/v) Coomassie Brilliant Blue R-250, 10% (v/v) acetic acid, 50% (v/v) methanol]. 2 μL of each sample was diluted five times with 10 mm Tris/HCl (pH 6.8) and then 2 μL of the diluted sample was dissolved in a sample loading buffer and was subjected to SDS/PAGE. The gel was transferred onto a polyvinylidene difluoride (PVDF) membrane, which was incubated at room temperature for 1 hour with TBST containing 5000-fold diluted tRFP antibody (Evrogen, Russia). The membrane was incubated at room temperature for one hour

in TBST containing 30,000-fold diluted horseradish peroxidase-labeled rabbit IgG secondary antibody. The immunoreactive bands were visualized with ECL Plus Western Blotting Detection Reagents (Amersham Biosciences). The signal intensity of the bands of Western blotting were calculated with Quantity One 1D Analysis Software (Bio-Rad Laboratories), in comparison with the intensity of rKFP-Red as a control.

Table S1. Absorption changes in absorption spectra (400 – 800 nm) for AgNP-embedded silk relative to native bare control silk under different conditions.

Mole ratio of $AgNO_3$ (@ 5 minutes)	0.3 mM	0.5 mM	0.7 mM	1.0 mM
(%)[a)]	15.6	32.5	67.2	96.4
Treatment time (@ 0.5 mM)	1 minute	5 minutes	10 minutes	20 minutes
(%)	15.9	32.5	84.5	95

[a)] Percentage changes with respect to bare control silk.

Table S2. Mechanical properties of bare native (control) silk fibers and AgNP-embedded silk fibers with different mole ratios of $AgNO_3$.

Sample[a)]	Average diameter of fibers (μm)	Maximum strain (%)	Maximum stress (MPa)	Young's modulus (GPa)
Native bare silk (Control)	9.8 ± 0.5[b)]	12.7 ± 3.9	383.6 ± 57.3	9.2 ± 0.8
AgNP-embedded silk (@ 0.5 mM and 5 minutes)	9.6 ± 0.6	12.9 ± 4.0	372.0 ± 48.8	8.7 ± 0.6
AgNP-embedded silk (@ 1.0 mM and 5 minutes)	9.7 ± 0.6	13.1 ± 4.2	360.2 ± 54.8	9.0 ± 0.8

[a)] For each silk cocoon, at least 15 single fibers were tested. [b)] Mean ± standard deviation. The Young's moduli are calculated from the first linear regime of the strain-stress curve before the first bend in Fig. S9.

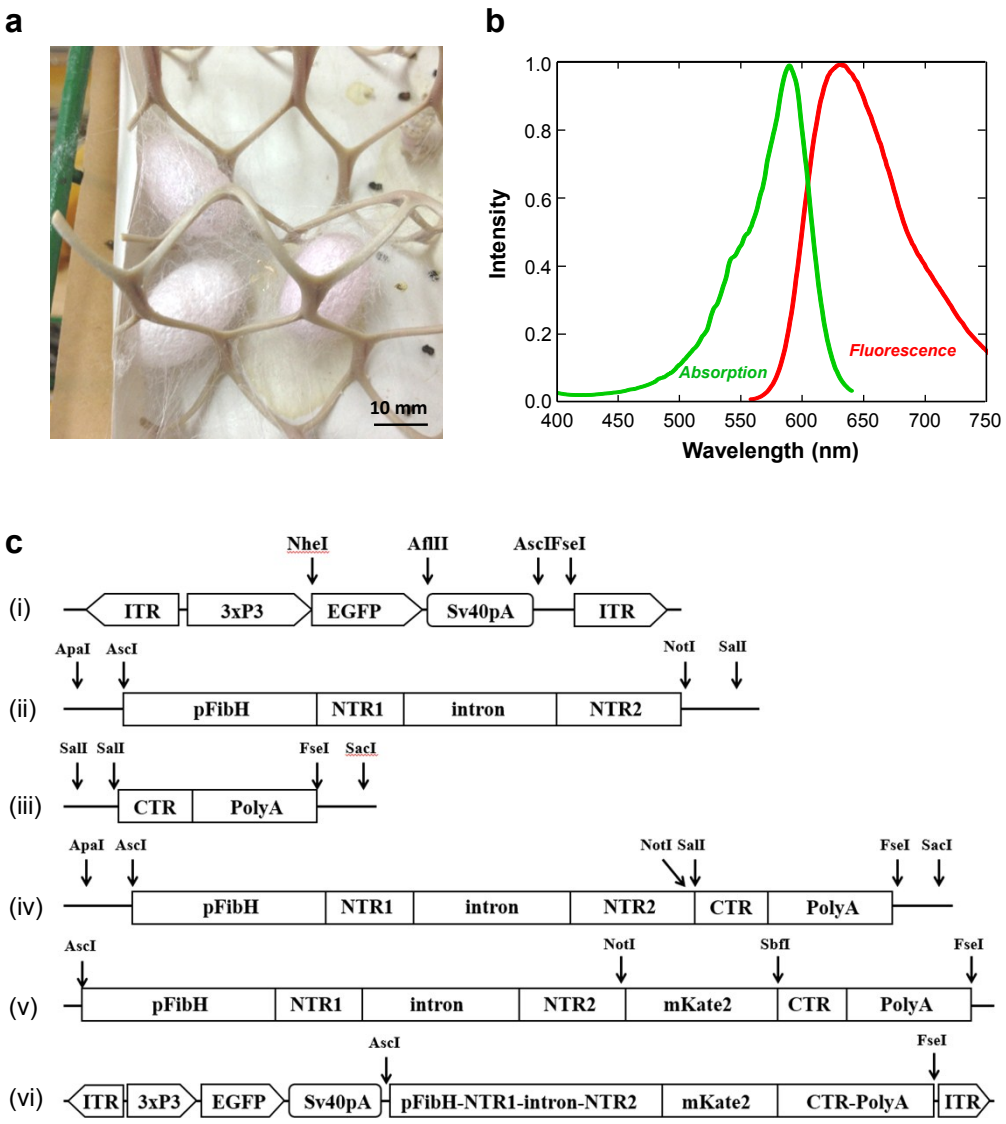

Fig. S1 (a) Photograph of the rearing environment for transgenic silkworms to produce mKate2 expressing silk cocoons. (b) Molar absorption and fluorescence spectra of far-red fluorescent mKate2 protein. (c) Transformation vector for germline transgenesis. (i) pBac-3xP3-EGFP. (ii) pGEMT-pFibH-NTR. (iii) pGEMT-CTR. (iv) pFibHNC-null. (v) pFibHNC-mKate2. (vi) p3xP3-EGFP-pFibH-mKate2. The nucleotide sequences of pFibH-NTR and CTD were derived from Genebank Accession No. AF226688. pFibH: fibroin heavy chain promoter domain (1124 bp), NTR1: N-terminal region 1 (142 bp), intron: first intron (871 bp), NTR2: N-terminal region 2 (417 bp), CTR: C-terminal region (179 bp), PolyA: poly(A) signal region (301 bp), EGFP: enhanced green fluorescent protein gene, mKate2: monomeric far-red fluorescent protein, ITR: inverted repeat sequences of *piggyBac* arms, 3xP3: 3xP3 promoter, and SV40: SV40 polyadenylation signal sequence. The restriction enzyme sites for the construction of recombinant vectors are indicated with the arrows.

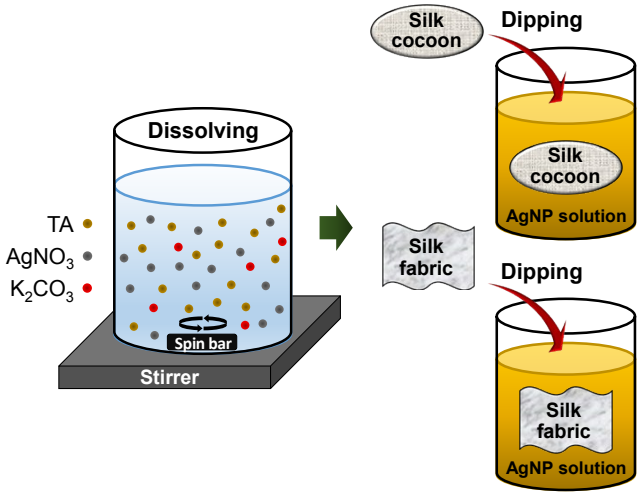

Fig. S2 Simplified schematic diagram of synthesizing AgNP-embedded silk via facile and green chemistry.

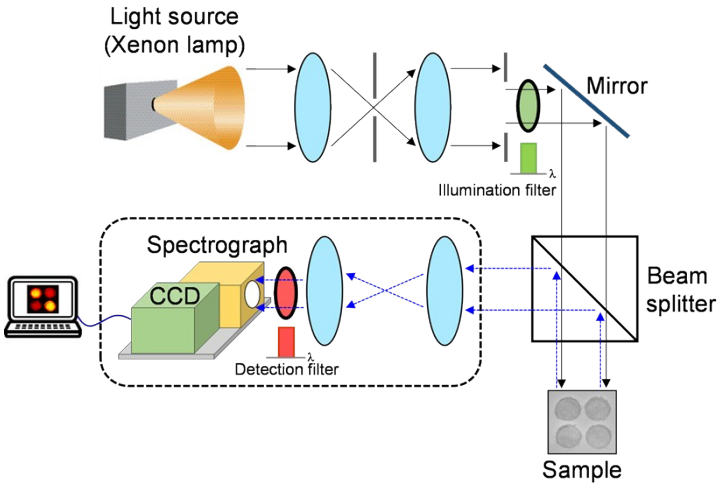

Fig. S3 Customized mesoscopic (between microscopic and macroscopic) imaging setup. This system provides a matrix of intensity as a function of x and y at each wavelength λ with a spectral resolution of 4 nm in a range of 400 – 800 nm. The imaging area of our mesoscopic imaging setup is ~ 15 mm × 15 mm with a pixel size of 50 μm × 50 μm.

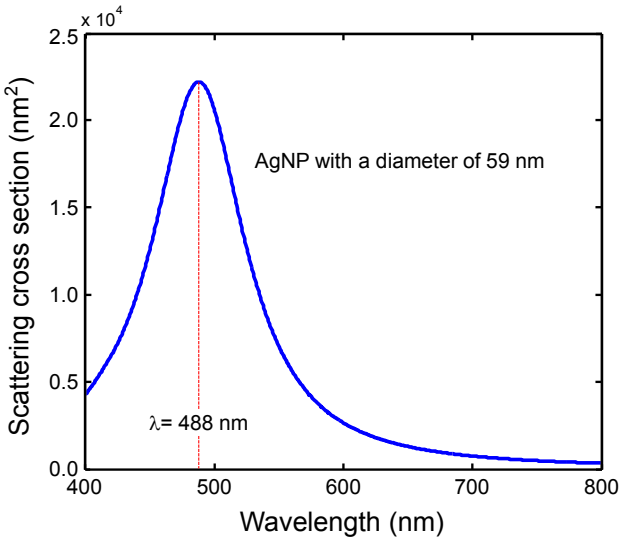

Fig. S4 Calculated scattering cross section of an AgNP inside silk with a diameter of 59 nm. The plasmon resonance occurs $\lambda = 488$ nm where the scattering cross section of AgNP is 8.1 times larger than the geometrical cross section. This simple example supports the use of RCM for directly visualizing AgNPs.

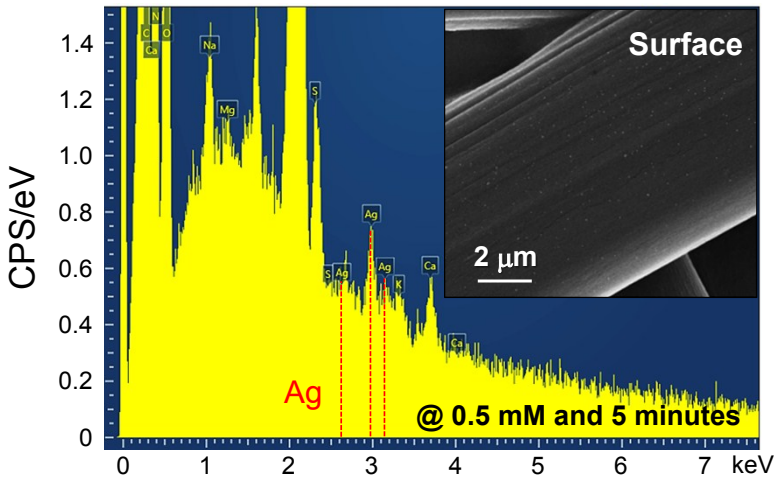

Fig. S5 EDX spectrum and SEM image on the surface of AgNP-embedded silk fibers with a low density of AgNPs (i.e., mole ratio of $AgNO_3$ = 0.5 mM and treatment time = 5 minutes), also confirming the presence of AgNPs on the surface, in addition to internalized AgNPs (Fig. 1).

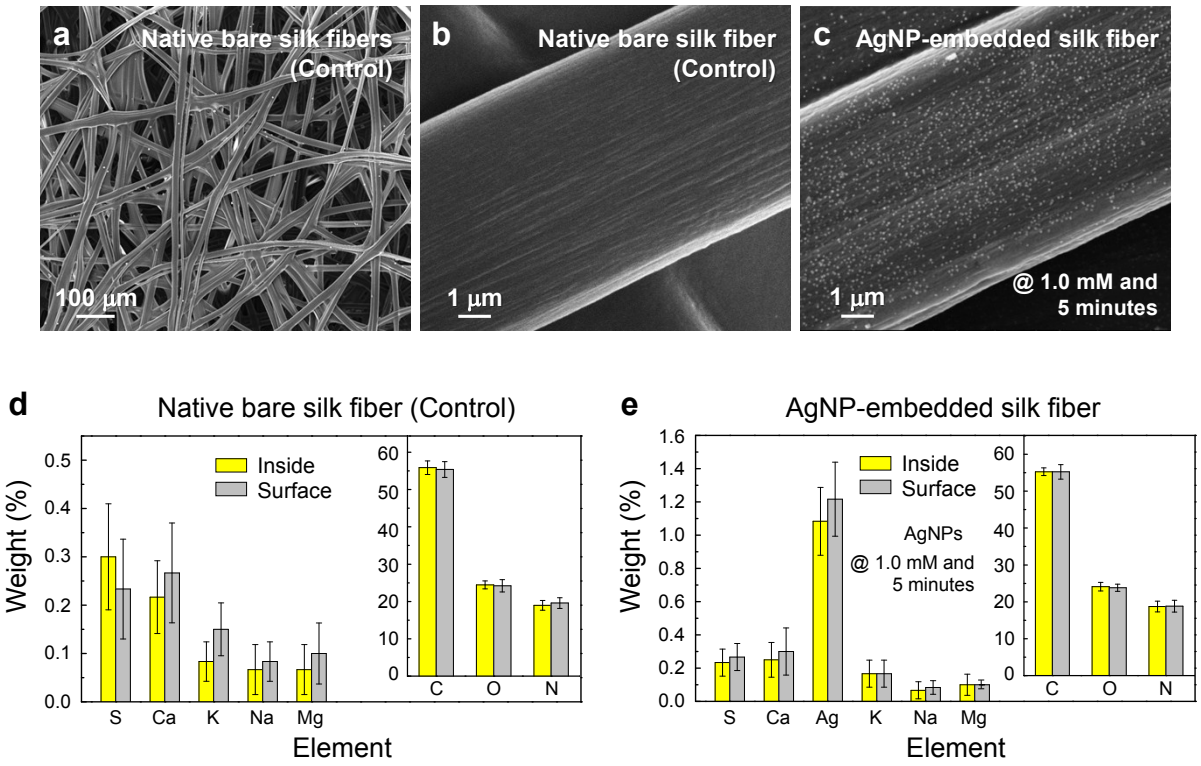

Fig. S6 SEM images of (a&b) native bare silk fibers (control) and (c) AgNP-embedded silk fiber synthesized under a relatively high-density condition (i.e., mole ratio of $AgNO_3$ = 1.0 mM and treatment time = 5 minutes). (d&e) Comparisons of EDX elements of native bare silk (control) and AgNP-embedded silk inside fibers and on the fiber surface. The native bare silk fibers do not show any element of Ag.

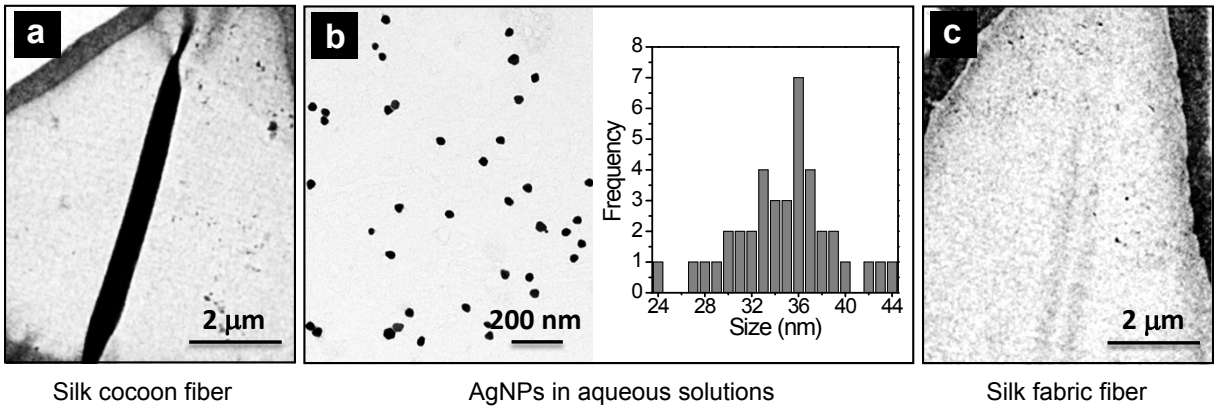

Fig. S7 TEM images of (a) AgNP-embedded fibers of silk cocoons, (b) isolated AgNPs synthesized in aqueous solutions (left) and TEM-derived size distribution of AgNPs (right), and (c) AgNP-embedded fibers of silk fabrics. All of the samples are prepared for low-density AgNPs at 0.5-mM $AgNO_3$ for five minutes. The sizes of sphere-like AgNPs synthesized in aqueous solutions are in a range of 24 − 44 nm, with a mean size of ~ 35 nm. The randomly distributed AgNPs are present inside fibers of both AgNP-embedded silk cocoons and fabrics.

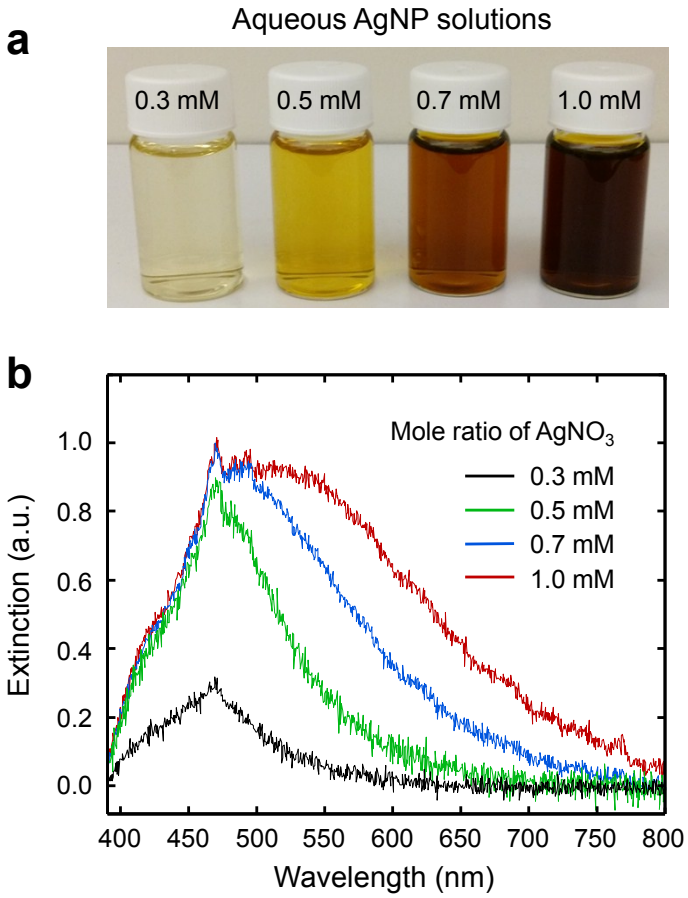

Fig. S8 (a) Photograph of aqueous AgNP solutions under different mole ratios of $AgNO_3$. (b) Measured extinction spectra of the corresponding AgNP solutions. Broad spectra indicates larger sizes of AgNPs with higher densities without the nanostructural frame of native silk.

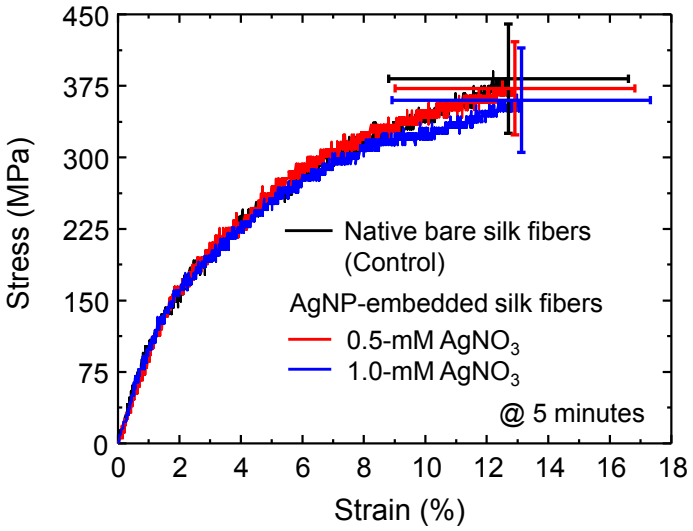

Fig. S9 Representative strain−stress curves of bare native (control) silk fibers and AgNP-embedded silk fibers with different mole ratios of $AgNO_3$. The error bars show the standard deviations of elongation at break (horizontal axis) and fracture strength (vertical axis).

a

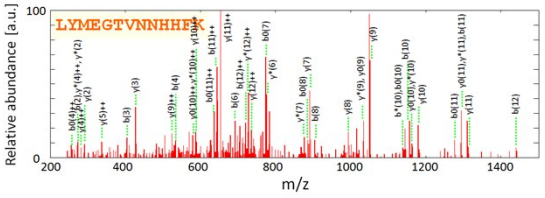

#	b	b++	b*	b*++	b0	b0++	Seq.	y	y++	y*	y*++	y0	y0++	#
1	114.1	57.55					L							13
2	**277.2**	139.1					Y	1478	**739.3**	1461	**730.8**	1460	730.3	12
3	**408.2**	204.6					M	**1315**	**657.8**	**1298**	**649.3**	**1297**	**648.8**	11
4	**537.2**	269.1			519.2	**260.1**	E	**1184**	**592.3**	**1167**	**583.8**	**1166**	**583.3**	10
5	594.3	297.6			576.2	288.6	G	**1055**	**527.8**	**1037**	519.2	**1036**	518.8	9
6	**695.3**	348.2			677.3	339.2	T	**997.5**	499.2	980.5	490.7	979.5	490.2	8
7	794.4	397.7			**776.4**	388.7	V	**896.4**	448.7	**879.4**	440.2			7
8	**908.4**	454.7	891.4	446.2	**890.4**	445.7	N	797.4	399.2	**780.3**	390.7			6
9	1023	512.2	1006	503.7	1005	503.2	N	683.3	**342.2**	666.3	333.7			5
10	**1161**	580.8	**1143**	572.2	**1142**	571.8	H	568.3	**284.7**	551.3	**276.1**			4
11	**1298**	**649.3**	1281	640.8	**1280**	**640.3**	H	**431.2**	216.1	414.2	207.6			3
12	**1445**	**722.8**	1428	714.3	1427	713.8	F	**294.2**	147.6	**277.2**	139.1			2
13							K	147.1	74.06	130.1	65.55			1

b

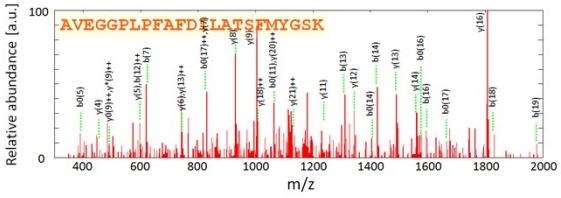

#	b	b++	b0	b0++	Seq.	y	y++	y*	y*++	y0	y0++	#
1	72.04	36.53			A							23
2	171.1	86.06			V	2363	1182	2346	1174	2345	1173	22
3	300.2	150.6	282.1	141.6	E	2264	**1133**	2247	1124	2246	1124	21
4	357.2	179.1	339.2	170.1	G	2135	**1068**	2118	1060	2117	1059	20
5	414.2	207.6	**396.2**	198.6	G	2078	1040	2061	1031	2060	1031	19
6	511.3	256.1	493.2	247.1	P	2021	**1011**	2004	1002	2003	1002	18
7	**624.3**	312.7	606.3	303.7	L	1924	962.5	1907	954	1906	953.5	17
8	721.4	361.2	703.4	352.2	P	**1811**	905.9	1794	897.4	1793	896.9	16
9	868.5	434.7	850.4	425.7	F	1714	857.4	1697	848.9	1696	848.4	15
10	939.5	470.3	921.5	461.2	A	**1567**	783.9	1550	775.4	1549	774.9	14
11	1087	543.8	**1069**	534.8	F	**1496**	**748.4**	1479	739.8	1478	739.4	13
12	1202	**601.3**	1184	592.3	D	**1349**	674.8	1332	666.3	1331	665.8	12
13	**1315**	657.8	1297	648.8	I	**1234**	617.3	1217	608.8	1216	608.3	11
14	**1428**	714.4	**1410**	705.4	L	1121	560.8	1104	552.3	1103	551.8	10
15	1499	749.9	1481	740.9	A	**1007**	504.2	990.4	**495.7**	989.4	**495.2**	9
16	**1600**	800.4	**1582**	791.4	T	**936.4**	468.7	919.4	460.2	918.4	459.7	8
17	1687	843.9	**1669**	**834.9**	S	**835.4**	418.2	818.3	409.7	817.4	409.2	7
18	**1834**	917.5	1816	908.5	F	**748.3**	374.7	731.3	366.2	730.3	365.7	6
19	**1981**	991	1963	982	M	**601.3**	301.1	584.2	292.6	583.3	292.1	5
20	2144	1073	2126	1064	Y	**454.2**	227.6	437.2	219.1	436.2	218.6	4
21	2201	1101	2183	1092	G	291.2	146.1	274.1	137.6	273.2	137.1	3
22	2288	1145	2270	1136	S	234.1	117.6	217.1	109.1	216.1	108.6	2
23					K	147.1	74.06	130.1	65.55			1

c

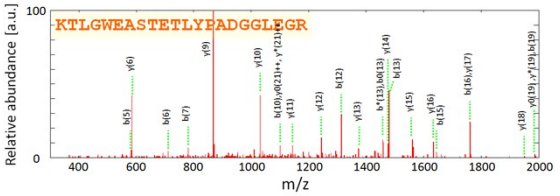

#	b	b++	b*	b*++	b0	b0++	Seq.	y	y++	y*	y*++	y0	y0++	#
1	129.1	65.05	112.1	56.54			K							22
2	230.1	115.6	213.1	107.1	212.1	106.6	T	2223	1112	2206	**1104**	2205	**1103**	21
3	343.2	172.1	326.2	163.6	325.2	163.1	L	2122	1062	2105	1053	2104	1053	20
4	400.3	200.6	383.2	192.1	382.2	191.6	G	2009	1005	**1992**	996.5	**1991**	996	19
5	**586.3**	293.7	569.3	285.2	568.3	284.7	W	**1952**	976.5	1935	967.9	1934	967.4	18
6	**715.4**	358.2	698.4	349.7	697.4	349.2	E	**1766**	883.4	1749	874.9	1748	874.4	17
7	**786.4**	393.7	769.4	385.2	768.4	384.7	A	**1637**	818.9	1620	810.4	1619	809.9	16
8	873.4	437.2	856.4	428.7	855.4	428.2	S	**1566**	783.4	1549	774.9	1548	774.4	15
9	974.5	487.8	957.5	479.2	956.5	478.7	T	**1479**	739.9	1462	731.3	1461	730.9	14
10	**1104**	552.3	1087	543.8	1086	543.3	E	**1378**	689.3	1361	680.8	1360	680.3	13
11	1205	602.8	1188	594.3	1187	593.8	T	**1249**	624.8	1232	616.3	1231	615.8	12
12	**1318**	659.3	1301	650.8	1300	650.3	L	**1148**	574.3	1131	565.8	1130	565.3	11
13	**1481**	740.9	**1464**	732.4	**1463**	731.9	Y	**1034**	517.7	1017	509.2	1016	508.7	10
14	1578	789.4	1561	780.9	1560	780.4	P	**871.4**	436.2	854.4	427.7	853.4	427.2	9
15	**1649**	824.9	1632	816.4	1631	815.9	A	774.4	387.7	757.3	379.2	756.4	378.7	8
16	**1764**	882.4	1747	873.9	1746	873.4	D	703.3	352.2	686.3	343.7	685.3	343.2	7
17	1821	910.9	1804	902.4	1803	901.9	G	**588.3**	294.7	571.3	286.1	570.3	285.7	6
18	1878	939.4	1861	930.9	1860	930.4	G	531.3	266.1	514.3	257.6	513.3	257.1	5
19	**1991**	996	1974	987.5	1973	987	L	474.3	237.6	457.2	229.1	456.3	228.6	4
20	2120	1061	2103	1052	2102	1052	E	361.2	181.1	344.2	172.6	343.2	172.1	3
21	2177	1089	2160	1081	2159	1080	G	232.1	116.6	215.1	108.1			2
22							R	175.1	88.06	158.1	79.55			1

d

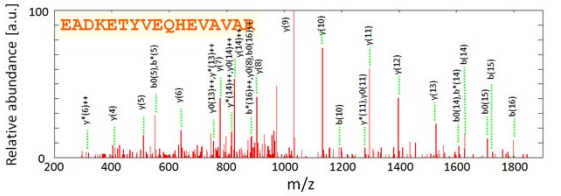

#	b	b++	b*	b*++	b0	b0++	Seq.	y	y++	y*	y*++	y0	y0++	#
1	130	65.53			112	56.52	E							17
2	201.1	101			183.1	92.04	A	1846	923.5	1829	914.9	1828	914.4	16
3	316.1	158.6			298.1	149.6	D	1775	887.9	1758	879.4	1757	878.9	15
4	444.2	222.6	427.2	214.1	426.2	213.6	K	1660	**830.4**	1643	**821.9**	1642	**821.4**	14
5	573.3	287.1	**556.2**	278.6	**555.2**	278.1	E	**1532**	766.4	1515	**757.9**	1514	**757.4**	13
6	674.3	337.7	657.3	329.1	656.3	328.6	T	**1403**	701.9	1386	693.3	1385	692.8	12
7	837.4	419.2	820.3	410.7	819.4	410.2	Y	**1302**	651.3	**1285**	642.8	**1284**	642.3	11
8	936.4	468.7	919.4	460.2	918.4	459.7	V	**1139**	569.8	1122	561.3	1121	560.8	10
9	1065	533.2	1048	524.7	1047	524.2	E	**1040**	520.3	1022	511.7	1022	511.3	9
10	**1195**	597.8	1177	589.2	1177	588.8	Q	**910.5**	455.7	893.4	447.2	**892.5**	446.7	8
11	1332	666.3	1315	657.8	1314	657.3	H	**781.4**	391.2	764.4	382.7	763.4	382.2	7
12	1461	730.8	1444	722.3	1443	721.8	E	**644.4**	322.7	627.3	**314.2**	626.4	313.7	6
13	1560	780.3	1543	771.8	1542	771.3	V	**515.3**	258.2	498.3	249.7			5
14	**1631**	815.9	**1614**	807.4	**1613**	806.9	A	**416.3**	208.6	399.2	200.1			4
15	**1730**	865.4	1713	856.9	**1712**	856.4	V	345.2	173.1	328.2	164.6			3
16	**1801**	900.9	1784	**892.4**	1783	**891.9**	A	246.2	123.6	229.1	115.1			2
17							R	175.1	88.06	158.1	79.55			1

Fig. S10 Tandem mass spectra of (a) 1827.88 m/z, (b) 1685.76 m/z, (c) 945.43 m/z, and (d) 843.43 m/z of mKate2 tryptic fragments and derived amino acid sequences.

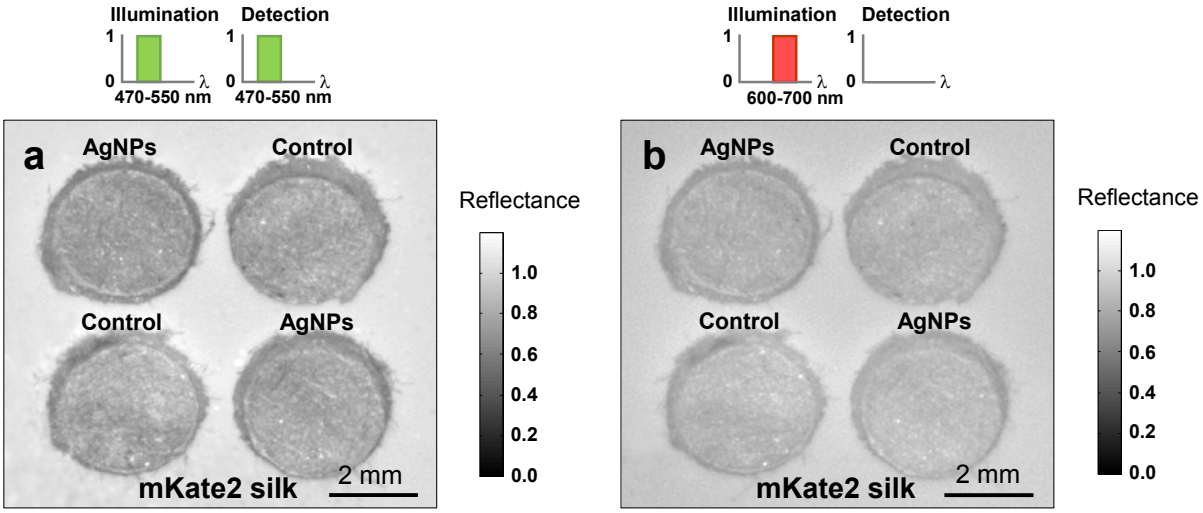

Fig. S11 (a&b) Reflectance images under two different illumination bands as illustrated on top. Changes in the scattering strength among different specimens are almost negligible, due to the low density of AgNPs. The specimens are placed on top of a white reflectance standard with a reflectivity of 99% (Labsphere SRS-99-010).

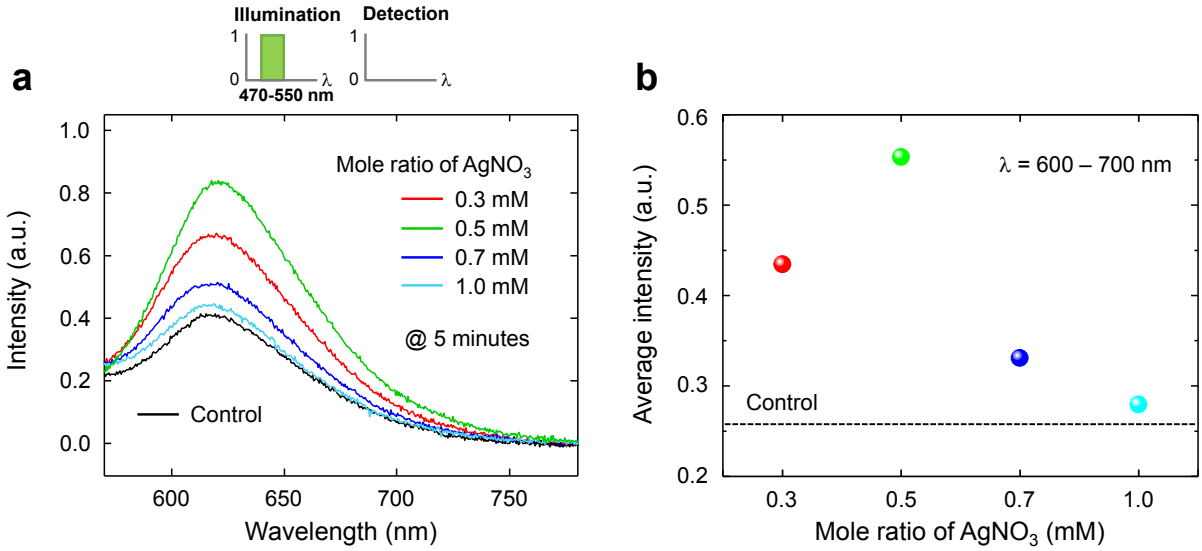

Fig. S12 (a) Emission spectra of AgNP-embedded mKate2 silk cocoons synthesized with different $AgNO_3$ mole ratios. (b) Photoluminescent intensity of the corresponding samples averaged by a bandwidth of $\lambda = 600 - 700$ nm. The dotted line in (b) is the average emission intensity of the control mKate2 silk cocoon. The synthesis condition of 0.5-mM $AgNO_3$ and 5-minute treatment time provides an optimal hybridization for plasmon-enhanced photoluminescence of mKate2 silk.

ESI reference

1. L. Y. Cai, H. L. Shao, X. C. Hu and Y. P. Zhang, *ACS Sustainable Chemistry & Engineering*, 2015, **3**, 2551-2557.
2. M. F. Pantano, A. Berardo and N. M. Pugno, *Scientific Reports*, 2016, **6**, 18222.
3. Q. Wang, C. Wang, M. Zhang, M. Jian and Y. Zhang, *Nano Letters*, 2016, **16**, 6695-6700.